한국항해항만학회지 제38권 제5호
J. Navig. Port Res. Vol. 38, No. 5 : 443-450, October 2014 (ISSN:1598-5725(Print)/ISSN:2093-8470(Online))
DOI : http://dx.doi.org/10.5394/KINPR.2014.38.5.443

The Numerical Study on the Flow Characteristics in Two-Dimensional Moonpool in Waves

Sang-min Lee · † Nam-Kyun Im*

** Dept. of Marine Science and Production, Kunsan National University, Kunsan 573-701, Korea*
† Division of Marine Transportation System, Mokpo National Maritime University, Jeonnam, 530-729, Korea

Abstract : *The objective of this study is to examine the nonlinear fluid characteristics near and inside a moonpool in various sea conditions. We estimate the flow of the free surface in a moonpool taking into account the viscosity effect and the hydrodynamic forces that affects a moonpool and hull through CFD calculations. The comparison of horizontal forces per wave length shows that the hydrodynamic force is greater for the long wave length than short wave length, and the greatest hydrodynamic force acts on the moonpool when the wave length is equal to the ship's length. The horizontal force decreases as the wave amplitude decreases, and the hydrodynamic force acting on the moonpool in $\lambda = LBP$ is 10 times that in $\lambda = LBP/3$. The free surface demonstrates the piston mode, in which it oscillates up and down while remaining essentially flat, and the rise of the free surface level increases as the wave length increases. We can assume that the hydrodynamic force acting on the moonpool increases owing to the effect of a strong vortex for $\lambda = LBP$ and owing to the rise of the free surface level for $\lambda = LBP \times 2$.*

Key words : *Moonpool, Hydrodynamic force, CFD, Free surface, Wave length, Wave amplitude*

1. Introduction

A moonpool is a structure used for divers, the launching or withdrawing equipment, and the installation of marine risers and cables needed for underwater missions. It is a circular or quadrilateral-shaped opening penetrating the deck to the bottom of a ship. Underwater missions can be executed via a moonpool in which the free surface is placid. However, the free surface in a moonpool is disturbed by moving with forward speed, the motion of a vessel, and sea conditions such as waves. In this case, a hull with a moonpool can be heavily damaged, and water can rise up to a working deck in a moonpool, which can greatly affect the security of a working site.

When a vessel moves in still water, flow disturbances occur owing to self-sustained oscillations where the formation and collision of the vortices caused by the separation and development of a shear layer lead to disturbances of the free surface(Rockwell and Naudasher, 1979; Lee et al., 2012). In order to determine the characteristics of these self-sustained oscillations, researchers conducted studies on the geometrical shape of the moonpool, the resonance period, and the correlation between the resistance performance and the fluid flow in a moonpool(Kim et al., 2006; Choi et al., 2011).

The flow in a moonpool, in addition to having an effect on hull structure, causes added resistance that has a significant effect on propulsion performance. The added resistance, which increases by up to 30% compared to still water, is directly related to the amplitude of the vertical oscillation of the flow in the moonpool(Van't Veer and Tholen, 2008). It also reduces sailing speed and increases fuel consumption.

There are two methods that can be considered for reducing the added resistance. The first is to inhibit the formation and development of vortices, and the second is to reduce the vertical movement of the flow. In order to reduce the flow behavior in a moonpool, which is a cause of increased resistance, studies have been conducted on mitigation devices such as wedges, plates, flaps, damping chambers, flanges, and openings, and they confirmed that these objects can be effectively applied within a specific range of sailing speeds(Fukuda, 1977; Gaillarde and Cotteleer, 2004; Hammargren and Törnblom, 2012).

Molin(2001) proposed a method in which one divides the movement of the water surface in a moonpool into a piston mode and sloshing mode, and computes the natural frequency of each mode, then constantly changes the width of a moonpool and the height of the water surface in a moonpool to estimate the resonant frequency at which the

† Corresponding author : namkyun.im@mmu.ac.kr 061)240-7177
* smlee@kunsan.ac.kr, 063)469-1814
Note) This paper was presented on the subject of "Flow Characteristics in Two-Dimensional Moonpool According to Wave Conditions" in spring conference of KINPR(Jinhae, Korea, 27th-28th June, 2013).

water surface rises the highest.

In order to understand the characteristics of a flow field owing to the self-movement in a moonpool, studies on forced heave motion of a two-dimensional floating body have been conducted by experiments, potential theories, and computational fluid dynamics (CFD) considered the viscosity effect(Faltinsen et al., 2007; Koo and Lee, 2010; Heo et al., 2011).

In the case that multiple structures, such as moonpools and side-by-side moored ships separated by narrow gap with free surfaces, are interpreted based on the linear potential theory, because the computed wave height and fluid force are overestimated(Lu et al., 2011; Kristiansen and Faltinsen, 2012), a numerical calculation should be performed by applying a method that can estimate nonlinear phenomena such as the viscosity effect and vortices occurring around a moonpool.

The causes of fluid flow occurring in a moonpool are thought of as the forward speed of a vessel moving in still water and the incident waves to a fixed vessel(Gaillarde and Cotteleer, 2004). The majority of studies to date include the change in a flow field that occurs when a vessel with a moonpool is sailing in still water and the added resistance due to the change in the flow field. However, a vessel actually on the sea is affected by many forms of waves with various wave heights and wave lengths.

Therefore, the first objective of this research is to examine the nonlinear fluid characteristics near and inside a moonpool in various sea conditions. The insights into these fluid characteristics can be expected to contribute to the development of design techniques that are appropriate for moonpools and fluid dampers. Furthermore, in this research, we estimated the flow of the free surface in a moonpool taking into account the viscosity effect and the hydrodynamic forces that affects a moonpool and hull through CFD calculations.

2. Numerical calculation

2.1 Calculation method

We have performed the numerical simulation based on the Marker and Cell (MAC) method. The governing equations which are the Navier-Stokes equation and the continuity equation in the case of two-dimensional, incompressible and viscous fluid are represented as follows,

$$\frac{\partial u}{\partial x}+\frac{\partial w}{\partial z}=0 \tag{1}$$

$$\frac{\partial u}{\partial t}+u\frac{\partial u}{\partial x}+w\frac{\partial u}{\partial z}=-\frac{\partial \phi}{\partial x}+\nu\left(\frac{\partial^2 u}{\partial x^2}+\frac{\partial^2 u}{\partial z^2}\right) \tag{2}$$

$$\frac{\partial w}{\partial t}+u\frac{\partial w}{\partial x}+w\frac{\partial w}{\partial z}=-\frac{\partial \phi}{\partial z}+\nu\left(\frac{\partial^2 w}{\partial x^2}+\frac{\partial^2 w}{\partial z^2}\right)+g \tag{3}$$

Here the Cartesian coordinate system is employed and velocity components are in respective direction. ϕ is the pressure divided by the fluid density and ν is the kinematic viscosity. The computational domain is discretized into a staggered rectangular inflexible mesh system with constant spacing in the horizontal direction while variable in the vertical one in order to have finer mesh near the body and the free surface.

An Euler explicit time stepping scheme is used for the time marching procedure with the time increment of $\Delta t=0.002$ seconds. The pressure field at the n-th time step is obtained by iteratively solving the Poisson equation which is derived by taking the divergence of velocities and set it to zero at the (n+1)th time step.

At the inflow boundary of the computational domain, a numerical wave-maker is established by prescribing the inflow velocities based on the linear theory. In the present study, the added dissipation zone method is employed as the wave absorbing condition at the outflow boundary. Inside the damping zone, the mesh size is gradually increased in the horizontal direction to provide additional numerical damping. The zero-normal gradient condition is given for the velocity and pressure at the outflow boundary.

At the free surface, the following fully nonlinear kinematic and dynamic conditions can be applied neglecting the viscous stress and surface tension,

$$\frac{D(\eta-z)}{Dt}=0 \tag{4}$$

$$P=P_0=0 \tag{5}$$

where D is the total derivative, η the wave height, z the vertical coordinate and P_0 the atmospheric pressure. Eq. (4) means that the particle on the free surface moves with the free surface.

The computational procedure is similar to the modified $TUMMAC\text{-}V_{WV}$ method which incorporate the subgrid-scale(SGS) turbulent model(Lee and Miyata, 1990).

2.2 Calculation condition

We chose as our research subject a sixth-generation drillship used for deep sea work because of its high load capacity and economic advantages. Table 1 shows the specifications of the model ship and wave conditions that were used for the numerical calculations in this research.

The purpose of this research is to examine and analyze the hydrodynamic forces and flow characteristics applied to a two-dimensional moonpool in various sea conditions. As shown in Fig. 1, waves with various properties are propagated from the left side. Numerical calculations were performed with three wave amplitudes of 1/4, 1/8, and 1/12 of the draft, and four wave lengths of 1/3, 1/2, 1, and 2 times the ship's length between perpendiculars (LBP). The range of Reynolds numbers between 7.0×10^6 and 1.7×10^7 was used for the calculation.

Table 1 Principal dimensions of 6th generation drillship (Fossli and Hendriks, 2008) and numerical calculation conditions

Parameter	Actual	Model (1/50)
Length (m)	228.0	4.56
Breadth (m)	42.0	0.84
Depth (m)	19.0	0.38
Draft (m)	12.0	0.24
Moonpool length (m)	25.6	0.512
Moonpool breadth (m)	12.5	0.25
Wave amplitude (m)	1.0, 1.5, 3.0	0.02, 0.03, 0.06
Wave period (sec.)	6.98, 8.55, 12.09, 17.09	0.99, 1.21, 1.71, 2.42

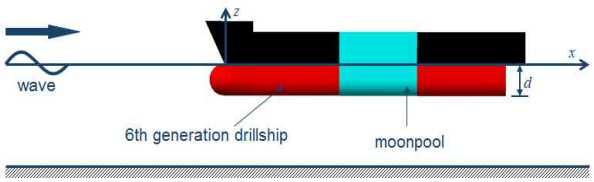

Fig. 1 Sketch definition of numerical setup

3. Added resistance in waves

3.1 Analysis of flow behavior

Figs. 2 - 5 show the change aspect of the flow field for different wave lengths with a wave amplitude equal to 1/4 of the draft($\zeta_a = 0.06m$). In the case of the shortest wave length (Fig. 2), because the wave energy hardly spreads, the flow inside the moonpool remained almost unchanged. However, as seen in Fig. 3($\lambda = LBP/2$), the flow was coming in from the bottom of the upstream submerged moonpool edge to the inside of the moonpool as the speed of the fluid changed; this also occurred to a lesser extent near the downstream submerged moonpool edge. Fig. 4 shows the change aspect of the flow field inside the moonpool with wave length equal to ship's length. It also shows that the largest vortex among different wave lengths disturbed the flow field. The results for this case, showing the greatest flow field change, will be discussed in detail later with Fig. 8. Fig. 5 shows the simulated results with the longest wave length, which was twice the ship's length($\lambda = LBP\times 2$). By comparing it with Fig. 4 ($\lambda = LBP$), it can be seen that a relatively large vortex occurred only at the downstream wall. This shows that because the decrease in energy owing to vortex shedding was relatively small, the free surface oscillated up and down, which caused a higher water surface rising effect (refer to Fig. 15).

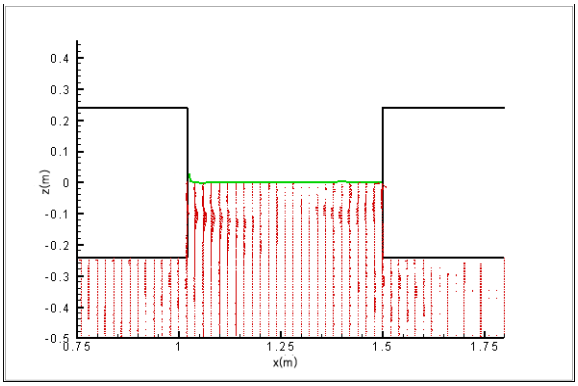

Fig. 2 Velocity vector for wave length $\lambda = LBP/3$ ($\zeta_a = 0.06m$)

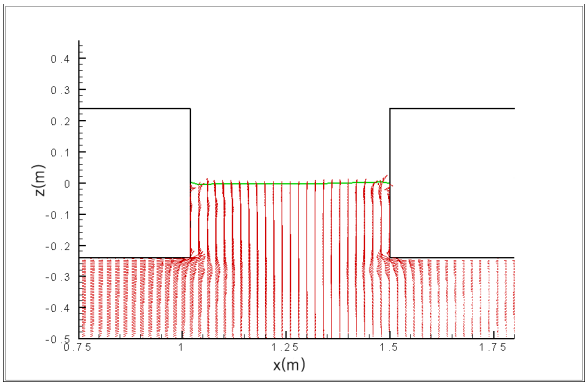

Fig. 3 Velocity vector for wave length $\lambda = LBP/2$ ($\zeta_a = 0.06m$)

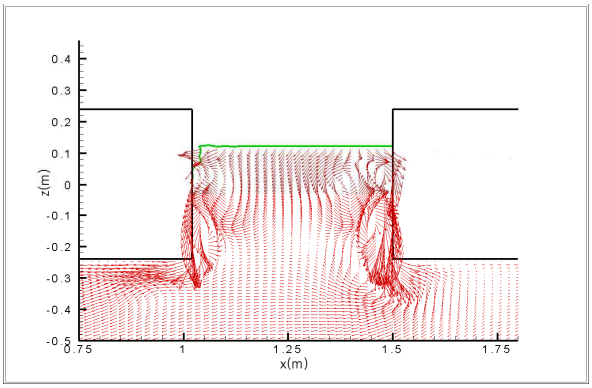

Fig. 4 Velocity vector for wave length $\lambda = LBP$ ($\zeta_a = 0.06m$)

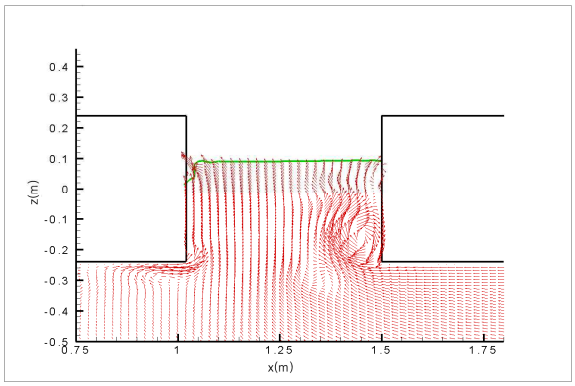

Fig. 5 Velocity vector for wave length $\lambda = LBP \times 2$ ($\zeta_a = 0.06m$)

Figs. 6 and 7 show the simulated results when the wave amplitudes were 1/8($\zeta_a = 0.03m$) and 1/12($\zeta_a = 0.02m$) of the draft, respectively. Vortices were created near the leading and trailing edges, and their size decreased as wave amplitude decreased and was the largest at the highest wave amplitude (Figs. 4 and 8). We presumed that these vortices affected the hydrodynamic forces acting on the moonpool, because relatively large vortices were generated compared to other wave lengths.

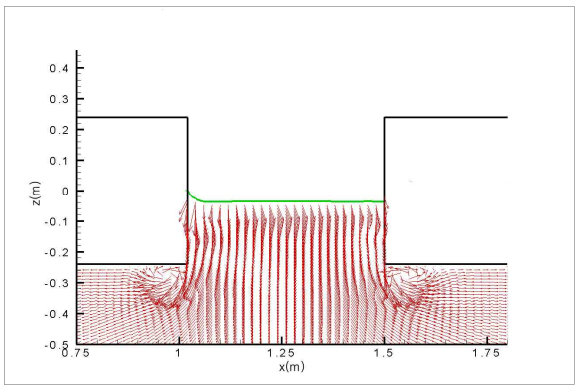

Fig. 6 Velocity vector for wave amplitude $\zeta_a = 0.03m$ ($\lambda = LBP$)

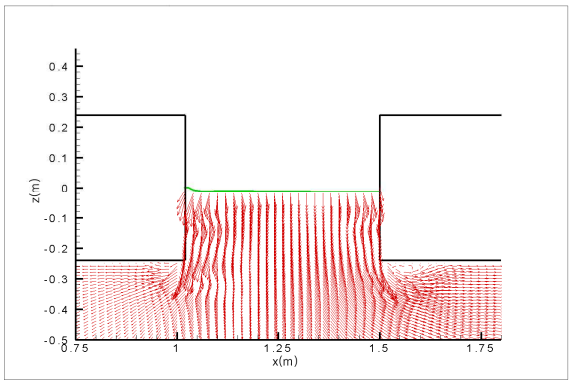

Fig. 7 Velocity vector for wave amplitude $\zeta_a = 0.02m$ ($\lambda = LBP$)

Fig. 8 shows the simulated results during a wave cycle. Vortices occurred at both ends of the moonpool and disturbed the flow field while rising up with the free surface along the wall of the moonpool, causing a change in pressure inside the moonpool. Therefore, we could predict that relatively greater hydrodynamic forces than in other cases were acting on the wall of the moonpool. A descending flow showed a repeating pattern that regenerated vortices at the upstream and downstream edges and resurged toward the inside of the moonpool.

Regarding the piston and sloshing modes, which increase resistance during sailing and decrease work safety, the sloshing mode is determined by the ratio of the draft (d) to the length of a moonpool (lm) and occurs in the following circumstances: $d/lm < 0.35 - 0.39$ (Van't Veer and Tholen, 2001), $d/lm < 0.66$ (Son et al., 2008), and $d/lm < 0.5$ (Fukuda and Yoshii, 2009). These different results seem to be caused by the different setups of the model simulations and the different shapes of the moonpools; as the length of the moonpool increases, the fluid flow is known to change from the piston mode to the sloshing mode(Hammargren and Törnblom, 2012). The ratio of the draft to the length of the moonpool for the drillship used for this research was 0.71, which is out of the range in which the sloshing mode occurs. As can be seen in the simulated results (Fig. 8), the free surface demonstrates the piston mode, in which it oscillates up and down while remaining essentially flat. We could confirm by the numerical calculation as mentioned above that the development of a vortex and the piston mode are quantitatively similar to the results of other studies.

3.2 Analysis of hydrodynamic force

Figs. 9 and 10 show the horizontal and vertical forces acting on the entire drillship at a wave amplitude of $\zeta_a = 0.06m$ and wave length of $\lambda = LBP/3$, and $\lambda = LBP$.

Considering the calculated results of a short wave length in Fig. 9, the hydrodynamic force acting on the leading body seems to determine the size of the fluid force acting on the entire drillship. This is because the hydrodynamic force caused by the wave affects only the bow and there is almost no wave exciting force at the stern of the ship. However, according to the calculated results when the wave length is equal to the ship's length (Fig. 10), a considerably large hydrodynamic force acts on the rear body of the ship, although it is not as large as the hydrodynamic force acting on the bow.

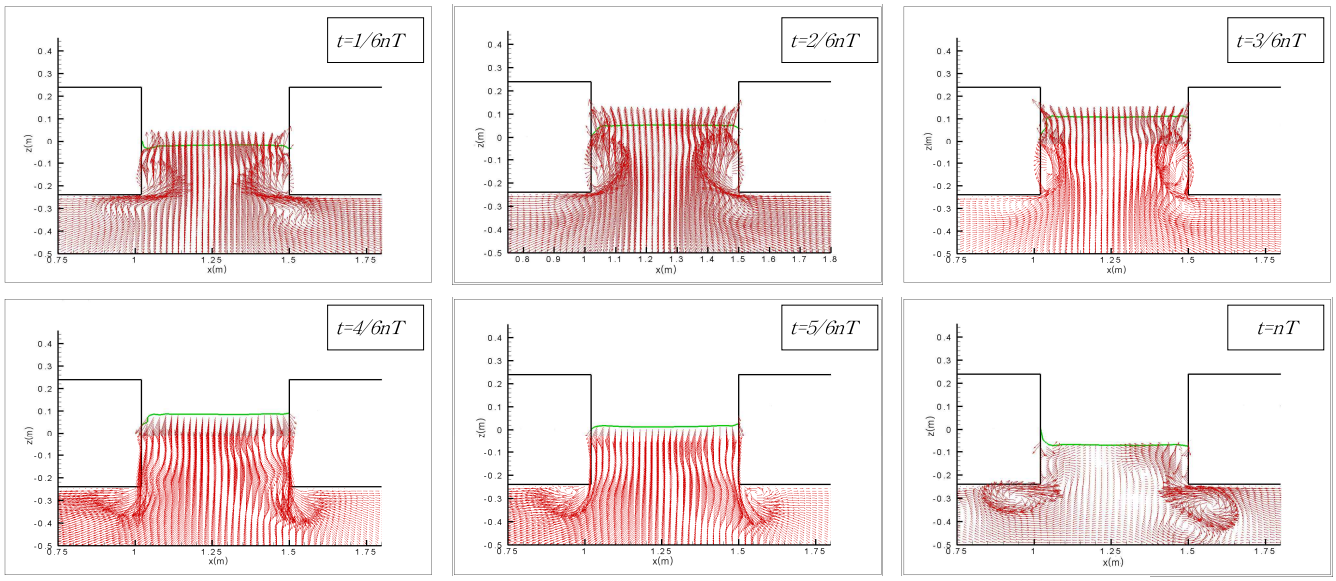

Fig. 8 Velocity vector field for wave length $\lambda = LBP$, wave amplitude $\zeta_a = 0.06m$

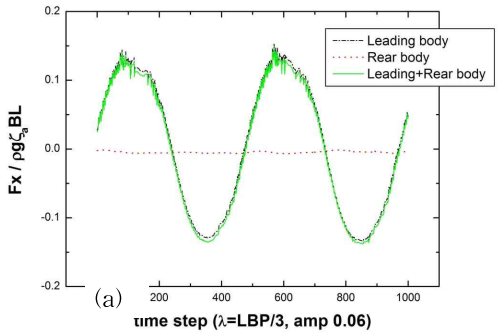

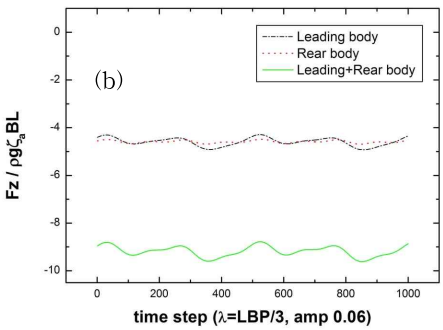

Fig. 9 Horizontal(a) and vertical(b) force on drillship for wave length $\lambda = LBP/3$, wave amplitude $\zeta_a = 0.06m$

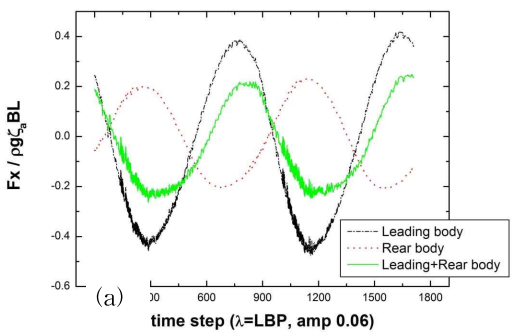

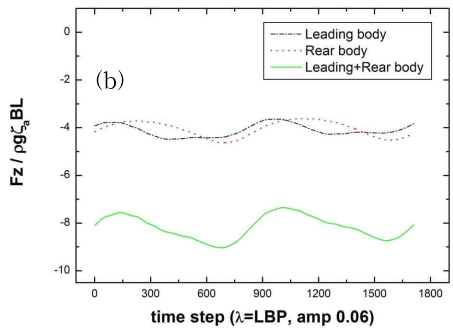

Fig. 10 Horizontal(a) and vertical(b) force on drillship for wave length $\lambda = LBP$, wave amplitude $\zeta_a = 0.06m$

Figs. 11 and 12 show the calculated results for the case of a horizontal force acting on the wall of the moonpool for wave length $\lambda = LBP/3$, and LBP. It can be seen that the greatest hydrodynamic force is acting on the moonpool when the wave amplitude is 1/4 of the draft($\zeta_a = 0.06m$). This horizontal force decreases as the wave amplitude decreases, and the hydrodynamic force acting on the moonpool in $\lambda = LBP$ is almost 10 times that in $\lambda = LBP/3$.

Figs. 13 and 14 show the results obtained through Fourier analysis to investigate the nonlinear effects of the hydrodynamic force acting on the moonpool of rear body. Considering the calculated results in Fig. 13 when the hydrodynamic force is the greatest ($\lambda = LBP$), it can be seen that the wave amplitude increases with the horizontal force. The interesting point noted from the calculated result in which the wave amplitude is the highest($\zeta_a = 0.06m$) is that the second-order component is greater than in the

other cases. This higher-order component is, as shown in Figs. 4 and 8, caused by the effect of nonlinear phenomena such as the formation and collision of relatively large vortices. Next, the comparison of horizontal forces per wave length (Fig. 14) shows that the hydrodynamic force is greater for the long wave length than short wave length, and the greatest hydrodynamic force acts on the moonpool when the wave length is equal to the ship's length ($\lambda = LBP$). In the case where the wave length is twice ship's length($\lambda = LBP \times 2$), it can be seen that higher-order component is larger owing to nonlinear phenomena such as vortices.

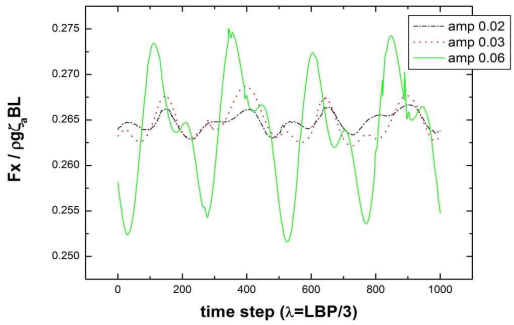

Fig. 11 Horizontal force on moonpool of rear body for wave length $\lambda = LBP/3$

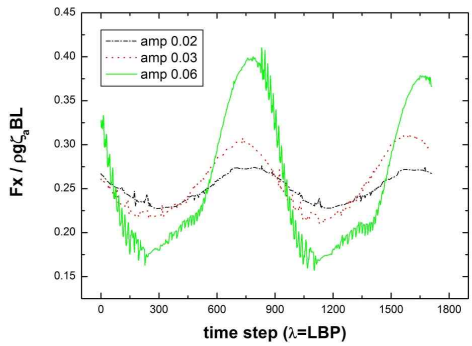

Fig. 12 Horizontal force on moonpool of rear body for wave length $\lambda = LBP$

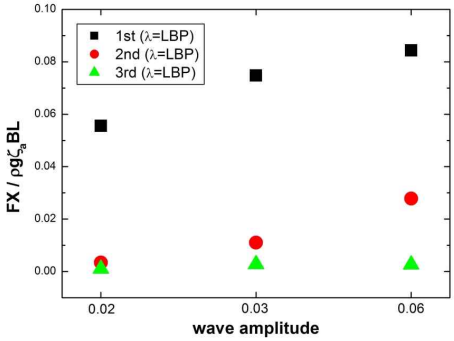

Fig. 13 Comparison of horizontal force on moonpool of rear body for wave length $\lambda = LBP$

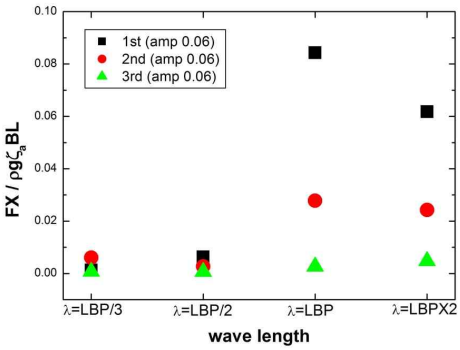

Fig. 14 Comparison of horizontal force on moonpool of rear body for wave amplitude $\zeta_a = 0.06m$

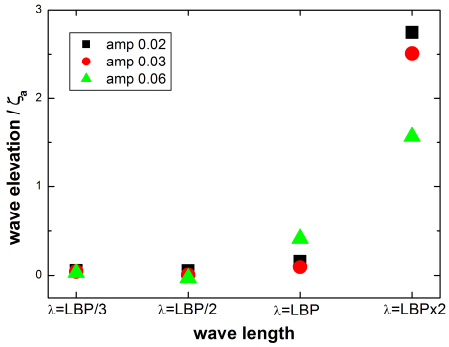

Fig. 15 Comparison of wave elevation in moonpool

Fig. 15 shows the rise of the average free surface level in the moonpool. As shown in the figure, the rise of the free surface level increases as the wave length increases. A previous study found that as the average free surface level in a moonpool increases, the added resistance acting on the body of a sailing ship increases(Choi et al., 2011). Therefore, when the wave length is double the ship's length, the hydrodynamic force acting on the moonpool increases along with the added resistance, and therefore, the effect of these phenomena on the propulsion performance of a vessel should be considered synthetically. Analyzing Figs. 13 - 15, we can assume that the hydrodynamic force acting on the moonpool increases owing to the effect of a strong vortex for $\lambda = LBP$ and owing to the rise of the free surface level for $\lambda = LBP \times 2$.

In the simulated results in Figs. 4 and 8, which show far greater hydrodynamic forces and stronger nonlinearity than other wave lengths and wave amplitudes, it can be seen that vortices rise up to almost 80% of the height of the free surface and exert a strong pressure on the moonpool while hitting the wall, which disturbs the flow field. This finding is similar to the results of an experiment(Lee et al., 2012) in which a greater part of the pressure fluctuation

acting on the moonpool of a ship moving in still water occurred at the midpoint of the depth of the moonpool rather than near the free surface. Because the pressure fluctuation acting on the wall of the moonpool has a strong correlation with the formation, development, and collision of vortices, we propose that CFD calculations, which simulate vortices better than the calculation method based on the potential theory, can be effectively applied to nonlinear hydrodynamic force calculations.

4. Conclusion

In this study, we have performed the numerical computation to examine the nonlinear fluid characteristics near and inside a moonpool in various sea conditions, and estimated the flow of the free surface in a moonpool taking into account the viscosity effect and the hydrodynamic forces that affects a moonpool and hull through CFD calculations.

The comparison of horizontal forces per wave length shows that the hydrodynamic force is greater for the long wave length than short wave length, and the greatest hydrodynamic force acts on the moonpool when the wave length is equal to the ship's length. The horizontal force decreases as the wave amplitude decreases, and the hydrodynamic force acting on the moonpool in $\lambda = LBP$ is 10 times that in $\lambda = LBP/3$. In the case $\lambda = LBP$ and $\lambda = LBP \times 2$, it can be seen that higher-order component is larger owing to nonlinear phenomena such as vortices.

The rise of the free surface level increases as the wave length increases. When the wave length is double the ship's length, the hydrodynamic force acting on the moonpool increases along with the added resistance, and therefore, the effect of these phenomena on the propulsion performance of a vessel should be considered synthetically. We can assume that the hydrodynamic force acting on the moonpool increases owing to the effect of a strong vortex for $\lambda = LBP$ and owing to the rise of the free surface level for $\lambda = LBP \times 2$.

References

[1] Choi, S. Y., Lee, Y. G., Jeong, K. L. and Ha, Y. J.(2011), "Reduction of added resistance by internal flow control in the moonpool of a drillship", Journal of the Society of Naval Architect of Korea, Vol. 48, No. 6, pp. 544-551.

[2] Faltinsen, O. M., Rognebakke, O. F. and Timokha, A. N.(2007), "Two-dimensional resonant piston-like sloshing in a moonpool", Journal of Fluid Mechanics, Vol. 575, pp. 359-397.

[3] Fossli, B. and Hendriks, S.(2008), "PRD 12,000 drill ship; increasing efficiency in deep water operations", Proc. of the 2008 International Association of Drilling Contractors/the Society of Petroleum Engineers Drilling Conference, pp. 1-17.

[4] Fukuda, K.(1977), "Behavior of water in vertical well with bottom opening of ship and its effects on ship motion", Journal of the Society of Naval Architects of Japan, Vol. 141, pp. 107-122.

[5] Fukuda, K. and Yoshii, Y.(2009), "Flow calculations in vertical cavity with free surface and bottom opening to water stream", The Journal of the Japan Society of Naval Architects and Ocean Engineer, Vol. 10, pp. 23-28.

[6] Gaillarde, G. and Cotteleer, A.(2004), "Water motion in moonpools empirical and theoretical approach", Proc. of ATMA-Association Technique Maritime et Aeronautique, No. 2435.

[7] Hammargren, E. and Törnblom, J.(2012), Effect of the moonpool on the total resistance of a drillship, Master Thesis, Chalmers university of technology.

[8] Heo, J. K., Park, J. C. and Kim, M. H.(2011), "CFD analysis of two-dimensional floating body with moonpool under forced heave motion", Journal of Ocean Engineering and Technology, Vol. 25, No. 2, pp. 36-46.

[9] Kim, D. J., Park, J. W., Kim, J. N. and Jeong, U. C.(2006), "An experimental study on the moonpool characteristics of a cleaning ship for ocean environment purification", Journal of Ocean Engineering and Technology, Vol. 20, No. 2, pp. 46-51.

[10] Koo, W. C. and Lee, K. R.(2010), "Motion analysis of two-dimensional floating body with moonpool using a numerical wave tank", Proc. of the Annual Spring Meeting the Society of Naval Architects of Korea, pp. 2133-2139.

[11] Kristiansen, T. and Faltinsen, O. M.(2012), "Gap resonance analyzed by a new domain-decomposition method combining potential and viscous flow DRAFT", Applied Ocean Research, Vol. 34, pp. 198-208.

[12] Lee, S. B., Han, B. W., Park, D. W., Ahn, Y. W., Go, S. C. and Seo, H. W.(2012), "Proper orthogonal decomposition of pressure fluctuations in moonpool", Journal of the Society of Naval Architect of Korea,

Vol. 49, No. 6, pp. 484-490.

[13] Lee, Y. G. and Miyata, H.(1990), "A finite-difference simulation method for 2D flows about bodies of arbitrary configuration", Journal of Society of Naval Architects of Japan, Vol. 167, pp. 1-8.

[14] Lu, L., Teng, B., Sun, L. and Chen, B.(2011), "Modeling of multi-bodies in close proximity under water waves - fluid forces on floating bodies", Ocean Engineering, Vol. 38, pp. 1403-1416.

[15] Molin, B.(2001), "On the piston and sloshing modes in moonpools", Journal of Fluid Mechanics, Vol. 430, pp. 27-50.

[16] Rockwell, D. and Naudasher, E.(1979), "Self-sustained oscillations of impinging free shear layers", Annual Review of Fluid Mechanics, Vol. 11, pp. 67-94.

[17] Son, H. J., Choi, S. H., Kim, M. H. and Hwangbo, S. M.(2008), "Drag reduction of recess type moonpool under vessels forward speed", Proc. of the ASME 27th International Conference on Offshore Mechanics and Arctic Engineering, OMAE2008-57118, pp. 143-148.

[18] Van't Veer, R. and Tholen, H. J.(2008), "Added resistance of moonpool in calm water", Proc. of the ASME 27th International Conference on Offshore Mechanics and Arctic Engineering, OMAE2008-57246, pp. 153-162.

Received 25 August 2014
Revised 30 October 2014
Accepted 30 October 2014